MHD Equilibrium Study of Noncircular Tokamak Reactor Plasmas

T.F. Yang and R.W. Conn

November 1975

UWFDM-152

FUSION TECHNOLOGY INSTITUTE

UNIVERSITY OF WISCONSIN

MADISON WISCONSIN

MHD Equilibrium Study of Noncircular Tokamak Reactor Plasmas

T.F. Yang and R.W. Conn

Fusion Technology Institute
University of Wisconsin
1500 Engineering Drive
Madison, WI 53706

http://fti.neep.wisc.edu

November 1975

UWFDM-152

Computational Study of MHD Equilibrium of Noncircular Tokamak Reactor Plasmas

by

Ted F. Yang

Robert W. Conn

November 1975

Nuclear Engineering Department

University of Wisconsin

Madison, Wisconsin 53706

Abstract

The MHD equilibrium and stability of noncircular tokamak plasmas limited by a separatrix is studied for two specific systems, a relatively small plasma with a current of 2.5 MA and a larger reactor size plasma with a current of 15.8 MA. The vertical field is produced by discrete external coils and no conducting shell is included. For the larger plasma, a stable equilibrium is found for a vertically elongated plasma with two stagnation points symmetrically located above and below the midplane as would be required for a system with a poloidal divertor. The plasma height to width ratio is 2, the plasma shape factor is 1.6 and the poloidal β is 1.2. The flux surfaces have triangular deformation which results from the need to maintain good curvature for the vacuum vertical field. The stability criteria relating to rigid motions, localized interchange modes, and kink modes are examined and found to be satisfied. An equilibrium shape for the smaller plasma is also found even for $\beta_\theta \sim 3.5$ (the aspect ratio is 5.6) and the stability criteria for localized modes are satisfied. However, the vacuum vertical field has the wrong curvature so that the system would require feedback for stabilization. The incorrect curvature of the vertical field is related to the engineering constraint that the coils cannot be placed arbitrarily close to the plasma which will especially be the case in reactor systems. Such coils are therefore not highly effective in controlling the plasma shape. Also discussed are the importance of such engineering constraints and the scaling of the two examples to different size tokamaks.

1. Introduction

Noncircular cross section tokamaks offer the potential for achieving higher values of total β, the ratio of particle to magnetic pressure, than circular plasmas with similar values of poloidal beta, β_θ, and stability factor, q.[1] The scaling is

$$\beta = \beta_p \left(\frac{S}{qA}\right)^2 \qquad \text{(I-1)}$$

where A is the aspect ratio and S is the perimeter of the noncircular cross section divided by the perimeter of the largest inscribed circle. From an economics viewpoint this could translate into a reactor systems of lower cost because lower toroidal magnetic fields would be required. Furthermore, noncircular cross section plasmas more optimally fill the available volume within a set of toroidal field coils designed with a constant tension, or "D", shape.[2] These advantages, however, will accrue only if plasma equilibrium and stability can be achieved at q values comparable to those in circular plasmas and this remains an important open question.

Additional difficulties are created by the potential needs of tokamak reactor systems. The use of a magnetic divertor for impurity control makes it necessary to find a stable equilibrium with null points on the plasma boundary. Also, discrete external coils rather than a conducting shell will be required and the location of these coils will be partially constrained by the need to place a 1 to 2 m thick blanket and shield region between the plasma and the coils. Thus, the external coils cannot be located arbitrarily close to the plasma chamber.

We study here the MHD equilibrium and stability of noncircular tokamak plasmas that are limited by a separatrix. The vertical field is produced by discrete external coils and no conducting shell is included. Two specific examples are used in the analysis, a relatively small noncircular plasma with a current of 2.5 MA suitable for two component tokamak operation[3,4] and a larger, reactor size system, UWMAK-III,[5] with a plasma current of 15.8MA.

II. MHD Equilibrium and Stability Theory

A. General Considerations

Future tokamaks and particularly tokamak power reactors will require discrete external coils rather than a conducting shell to keep the plasma in equilibrium. The required vacuum vertical field generated by such coils can be estimated in many ways. For example, a virtual shell can be placed around the plasma and, at equilibrium, one can replace the resulting image currents by a set of discrete coils.[6] One then iterates on this procedure until a new equilibrium configuration is determined using only discrete coils. Alternatively, one can estimate the required vacuum field strength on the midplane by using the formula[7,8] for circular tokamaks,

$$B_{\perp} = \frac{\mu_o I_\phi}{4 R} \left(\ln \left(\frac{8R}{a}\right) + \frac{1i}{2} + \overline{\beta}_\theta - \frac{3}{2} \right)$$

where

$$1i = \frac{1}{\pi a^2 B_\theta^2(a)} \int_o^a B_\theta^2(r)\, 2\pi r dr$$

The currents and locations of the external coils must then be adjusted until an equilibrium is found which satisfies additional constraints placed on the size and shape of the plasma and the decay index of the vacuum field. We find this second method more convienent to use in connection with studies on systems that include a poloidal divertor.

The equilibrium vertical field required for a noncircular, elliptical plasma of small eccentricity and uniform current density is[9]

$$B_{\perp} = \frac{\mu_o I_\phi}{4\pi R_o} \{\ln \frac{8R_o}{a} + \overline{\beta_\theta} - \frac{5}{4} - \frac{R-R_o}{R_o} [\frac{3}{4} \ln \frac{8R_o}{a} - \frac{17}{16} + \frac{R_o^2}{a^2} (1- \frac{b}{a})]\} \quad (1)$$

where R_o is the major radius, 2a is the plasma width, 2b is the plasma height and the average poloidal beta is defined as

$$\overline{\beta_\theta} = \frac{<P>}{\frac{B_\theta^2}{2\mu_o}} \quad . \quad (2)$$

The shift of the magnetic axis from the geometrical center is an important quantity and, in the large A limit, is approximately given by

$$\Delta_m = \frac{4\pi a^2}{2\mu_o I_p} B_{\perp} \quad . \quad (3)$$

Another important quantity is the decay index of the transverse field. For noncircular cross section and small β_θ, the decay index is given by

$$n = \frac{3}{4} \frac{\ln \frac{8R_o}{a} - \frac{17}{12}}{\ln \frac{8R_o}{a} + \overline{\beta_\theta} - \frac{5}{4}} + \frac{\frac{R_o^2}{a^2}(1 - \frac{b}{a})}{\ln \frac{8R_o}{a} + \overline{\beta_\theta} - \frac{5}{4}} \quad (4)$$

and we require $n > 0$ at the magnetic axis for stability with respect to radial and vertical displacements.[10] The condition $n > 0$ is valid only for $\frac{b}{a}$ small and R_o/a large, but it is sufficient for our purposes to know the field at the magnetic axis in order to estimate the current in the external coils.

B. MHD Equilibrium Calculations

The MHD equilibrium for anaxisymmetric system can be determined by solving the usual equation for the flux fuction Ψ which satisfies

$$X \frac{\partial}{\partial X} \left(\frac{1}{X} \frac{\partial \Psi}{\partial X} \right) + \frac{\partial^2 \Psi}{\partial Z^2} = -X J_\phi \quad , \tag{5}$$

where

$$J_\phi = X \frac{dp}{d\Psi} + \frac{R_o B_o^2}{X} g \frac{dg}{d\Psi} \quad . \tag{6}$$

The magnetic field has been decomposed into poloidal and toroidal components using

$$\vec{B} = B_o \left[f(\psi) \vec{\nabla\phi} X \vec{\nabla\psi} + R_o g(\psi) \vec{\nabla\phi} \right] \quad . \tag{7}$$

The coordinates R, ϕ and Z are the axisymmetric coordinates, ϕ is the ignorable variable and X is the distance from the symmetric axis. ψ represents an arbitrary surface lable and Ψ is the poloidal flux inside a magnetic surface.

The MHD study group at the Princeton Plasma Physics Laboratory[11] have developed a general computational program to solve equation (5) in which the plasma boundary is determined self consistently with the location of external coils. This program has been used for the studies presented in this paper. A square of arbitrary size is used as an outer boundary for the problem and the boundary conditions on this border are fixed by specifying the current in the external coils. As such, the procedure does not require the use of a conducting external boundary. The plasma boundary can be fixed by a limiter or a separatrix. The program evaluates $q(\Psi)$, $\beta_\theta(\Psi)$ and β_θ from the formulae:[12,13]

$$q(\psi) = \frac{f}{2\pi}\oint \frac{dl}{|\nabla\Psi| X} \quad , \tag{8}$$

$$\beta_\theta(\psi) = \frac{2\pi P}{\left\langle \frac{|\nabla\Psi|^2}{R^2} \right\rangle} \tag{9}$$

$$\overline{\beta_\theta} = \frac{\int P \frac{dv}{d\Psi} d\Psi}{\int^{\Psi} P \frac{dv}{d\Psi} d\Psi - R_o^2 B_o^2 \int^{\Psi} vg \frac{dg}{d\Psi} \left\langle \frac{1}{X^2} \right\rangle d\Psi} \tag{10}$$

Here,

$$V = 2\pi \int^{\Psi} d\Psi \oint \frac{X dl}{|\nabla\Psi|} \quad , \tag{11}$$

and

$$\frac{dV}{d\Psi} = 2\pi \oint \frac{dl}{|\nabla\Psi|} \quad . \tag{12}$$

The nonlinear equation (5) is solved by prescribing the functions $P(\Psi)$ and $g(\Psi)$ in equation (6). For the case of a reactor size system, the form of these functions has a significant effect on the equilibrium and stability of the plasma and warrants some discussions. If we choose

$$P(\Psi) = P_o \left(\frac{\Psi_* - \Psi}{\Psi_* - \Psi_o} \right)^{\alpha_1} \tag{13}$$

and

$$g(\Psi) = \left[1 - g_p \left(\frac{\Psi_* - \Psi_o}{\Psi_* - \Psi_m} \right)^{\alpha_2} \right] \quad , \tag{14}$$

the plasma current, $j_\phi(\Psi)$, has the form

$$j_\phi(\Psi) = - \frac{X_o P_o \alpha_1}{\Delta\Psi} \left(\frac{\Psi_* - \Psi}{\Delta\Psi} \right)^{\alpha_1 - 1} + \frac{\alpha_2 R_o^2 B_o^2}{\Delta\Psi X} g_p \left(\frac{\Psi_* - \Psi}{\Delta\Psi} \right)^{\alpha_2 - 1}$$

$$+ \frac{\alpha_2 R_o^2 B_o^2}{\Delta\Psi X} g_p^2 \left(\frac{\Psi_* - \Psi}{\Delta\Psi} \right)^{2\alpha_2 - 1} \quad , \tag{15}$$

where $\Delta\Psi = \Psi_* - \Psi_m$ and Ψ_*, Ψ_m are the flux at the plasma surface and magnetic axis. The constant g_p is varied until Ψ converges. On the other hand, if one chooses α_1 and $\alpha_2 = 1$, $p'(\Psi)$ and $g'(\Psi)$ are independent of Ψ and $j_\phi(\Psi)$ is given by

$$j_\phi(\Psi) = - \frac{X P_o}{\Delta\Psi} + \frac{R_o^2 B_o^2}{X\Delta\Psi} g_p + \frac{R_o^2 B_o^2}{X\Delta\Psi} \left(\frac{\Psi_* - \Psi}{\Delta\Psi} \right) g_p^2 \quad . \tag{16}$$

Thus, $j_\phi(\Psi)$ is nearly a linear function of R when $g_p < 1$. This however is not a desirable profile and does not appear to be consistent with present tokamak experiments. If we set $\alpha_1 = 2$ and $\alpha_2 = 1$, then

$$j_\phi(\Psi) = - \frac{2X P_o}{\Delta\Psi} \left(\frac{\Psi_* - \Psi}{\Delta\Psi} \right) + \frac{R_o^2 B_o^2}{X\Delta\Psi} g_p + \frac{R_o^2 B_o^2}{X\Delta\Psi} \left(\frac{\Psi_* - \Psi}{\Delta\Psi} \right) g_p^2 \tag{17}$$

The current profile is now nearly parabolic in r. However, for $\overline{\beta_\theta} > 2.0$, it is found that the safety factor becomes less than 1 near the magnetic axis. After further study, we find that values of α_1 and α_2 in the neighborhood of 1.4 are optimum.

C. Stability Analysis

The stability of the plasma with respect to rigid motions (vertical and radial displacements and flipping), localized interchange modes of both the resistive and ideal types, and general kink modes have each been considered.

1. Rigid Motions

We have found that one can often obtain large elongated plasmas of approximately elliptical shape with $\frac{b}{a} > 2$ and $S \simeq 1.8$ for which $q(\Psi) > 1$ and the plasma is stable against localized modes but which nevertheless has the wrong curvature associated with the vacuum vertical field. It is therefore unstable to rigid displacements and it is typically a major effort to arrange

the external coils such that the decay index, n, at the magnetic axis, R_m is greater than zero.

A detailed study has recently been made by Rebhan.[14] The necessary and sufficient criteria for stability with respect to any arbitrary rigid perturbation b_ξ are given as

$$\oint \frac{R\Psi_z}{|\nabla\Psi|} P_z^* \, dl + \frac{1}{2\pi} \int_s \vec{B} \cdot \vec{b}_\xi \vec{e}_\xi \cdot d\vec{s} = 0 \tag{18}$$

$$\oint \frac{R\Psi_R}{|\nabla\Psi|} P_R^* \, dl \geq 0 \tag{19}$$

and $$\oint \frac{R(R\Psi_z - Z\Psi_R)}{|\nabla\Psi|} (R P_z^* - Z P_R^*) dl \geq 0 \quad . \tag{20}$$

P* represents the equilibrium pressure while subscripted values of Ψ and P imply derivatives. These general criteria can be evaluated numerically and the stability can be cast in terms of critical values for the parameters, $e_{cr} \equiv \frac{b}{a}$, and q. Assuming a parabolic pressure profile, elliptical flux surfaces with triangular deformation, and constant values of $P'(\Psi)$ and $g(\Psi)g'(\Psi)$, Rebhan obtained the critical value of q, designated q_h, for stability with respect to horizontal displacement as

$$\lim_{A \to \infty} q_h = \frac{1}{\sqrt{2}} \quad . \tag{21}$$

He also found the critical q value, denoted q_f, for stability against flipping of the plasma ring as

$$\lim_{A \to \infty} q_f = 1 \quad . \tag{22}$$

The values of q_h and q_f tend to decrease as Λ decreases. The plasma is stable if q is greater than q_h and q_f. The existence of a critical q is to be expected from the fact that horizontal displacement and flipping are special kink modes and q must be kept above one to satisfy the Kruskal-Shafranov limit[15,16] and to obtain stability with respect to other kink modes. As such, no additional precautions need be taken. The criterion (18) can be reduced to[14]

$$C_{vert} = \oint \{\frac{1}{R|\nabla\Psi|}\left[-\Psi_R\Psi_{RR} + \frac{\Psi_Z\Psi_R}{R} + \Psi_R\Psi_{RZ} \right] + Y\} \Psi_z dl \geq 0 \qquad (23)$$

for vertical displacements, where $y = (\vec{e}_\theta \times \vec{n}).\vec{b}_\xi$.

2. Localized Modes

The criteria for stability with respect to the localized interchange modes are,[17,18] for idealized modes,

$$D_I = D + H\frac{1}{4} < 0$$

and for resistive modes,

$$D_R = D + H^2 < 0 \quad .$$

The parameters D and H are defined by

$$D \equiv \frac{\langle B^2/|\nabla V|^2\rangle}{\Lambda^2}\left[J'\phi''-I'\Psi'' + \frac{\langle\sigma B^2\rangle}{\langle B^2\rangle} + P'^2\left\langle\frac{1}{B^2}\right\rangle + \left\langle\frac{\sigma^2B^2}{|\vec{\nabla}V|^2}\right\rangle - \frac{\langle\sigma B^2/|\vec{\nabla}V|^2\rangle^2}{\langle B^2/|\vec{\nabla}V|^2\rangle}\right.$$

$$H \equiv \frac{\langle B^2/|\vec{\nabla}V|^2\rangle}{\Lambda}\left[\frac{\langle\sigma B^2/|\vec{\nabla}V|^2\rangle}{\langle B^2/|\vec{\nabla}V|^2\rangle} - \frac{\langle\sigma B^2\rangle}{\langle B^2\rangle}\right] \quad ,$$

where $\Lambda \equiv \phi'\Psi'' - \Psi'\phi''$ and $\sigma \equiv \vec{J}\cdot\vec{B}/B^2$. ϕ and Ψ are the toroidal and poloidal field flux functions and J and I and the toroidal and poloidal current fluxes, respectively. Primes denote derivatives with respect to the volume, V, and

brackets denote field line averages.

3. General Kink Modes

The stability with respect to kink modes may be insured by examining the q values and β. If the safety factor $q > 1$, the well-known Kruskal-Shafranov limit[15,16] is that all "m" modes are stabilized and the critical β for stability is $\beta = \varepsilon^2$, where $\varepsilon = \frac{a}{R}$, the inverse aspect ratio. A detail stability study by Freidberg[19] based on a sharp boundary model shows that the critical β_θ increases due to ellipticity and decreases due to triangularity. A value of this critical beta will be estimated from the results of Freidberg and used to estimate the stability against kink modes of the specific examples discussed next.

III. Calculation for Specific Tokamak Designs

A. UWMAK-III

UWMAK-III[5] is a conceptual design for a noncircular tokamak power reactor system with characteristic parameters as listed in table I. A cross sectional view is shown in Fig. 1. For this large system, the vacuum field calculated from Eqn. (3) is $B_\perp = 0.77T$ and the shift of magnetic axis calculated from eqn. (3) is $\Delta_m = 1.85m$. The decay index for mildly elliptical cross-sections is 0.34. The external coils were arranged in such a way that $B_\perp = 0.77T$ and $n > 0$ at $R_m = 10.0$ m.

Fig. 2 is a detailed flux plot for the equilibrium plasma in UWMAK-III and Fig. 3 shows the vacuum vertical field. Table II is a list of the locations and the currents in all the discrete external vertical field coils. As can be seen, the plasma cross section is vertically elongated with two stagnation points on the boundary that are symmetrically located above and below the median plane.

The stagnation points are fixed by the coil D_o. For reasons related to the overall conceptual design of the device, we have required that the plasma surface intersect the midplane at R_1 = 5.4m and R_2 = 10.8m. The stagnation point has been placed at a height above the midplane such that b ≃ 2a.

Two virtual limiters were placed at R=5m and R=11.5m to specify the initial size of the plasma at the beginning of the calculation. The parameters α_1 and α_2 were initially set at 1.4 for the reasons discussed in section II. The calculational sequence is to vary the locations and the currents in the external coils and the peak pressure, P_o, until an equilibrium is found with $\beta_\theta \cong 2.2$, $q(\Psi) > 1$ and the decay index $n > 0$. The parameters α_1 and α_2 are then varied until an optimum solution is found.

The two dimensional toroidal current density distribution is shown in Fig. 4 while the pressure and current profiles are shown in Fig. 5 as a function of R on the midplane. The magnetic axis is at ~ 9.0m, which is a shift outward of 0.9m from the plasma geometric center. The toroidal current, j_ϕ, peaks at R_j = 10.0m and we refer to this location as the toroidal current axis. It is interesting to note that the current axis is shifted outward beyong the magnetic axis by about 1 m. The vacuum vertical field at R_m=9.0 is $B_\perp \cong$ 0.7 T. This last value shows that formula (3) gives a reasonably accurate prediction for $B_\perp$ and is useful as an initial guess. In Fig. 5, surface Ψ = -0.130 is a flux surface near the magnetic axis while Ψ = -0.054 is the surface closest to the separatrix. Turning now to the stability problems, the vacuum field for UWMAK-III shown in Fig. 3 has good curvature to the right of the magnetic axis and bad curvature to the left. It seems clear that only for circular or mildly non-circular plasmas can the vacuum field have good curvature throughout the entire plasma cross section. However, the decay index criterion $n > 0$ is valid for circular plasmas of large aspect ratio. In general, it will be necessary to

calculate detailed spectra in order to understand the plasma stability with respect to small perturbations using a ΔW formation. This will be possible only when a ΔW code becomes operational.[20]

One important observation which can be made is that the large triangularity of the plasma shape is a result of forcing the vertical field to have good curvature in the region to the right of the magnetic axis. The decay index n is small but positive. To obtain larger values of n would require a reduction in the height to width ratio, $\frac{b}{a}$, and shape factor S, i.e., a reduction in the ellipticity. When n becomes negative, the triangularity is reduced and the plasma becomes more and more elliptical. This agrees with many theoretical predictions that vertically elongated plasma cross sections with large triangularity are more stable[14,21]. Obviously the plasma will be more stable when n becomes larger until it reaches some maximum n value. The present plasma for UWMAK-III gives an elongation factor, $e = 2$ and a shape factor, $S = 1.6$. Since the vacuum vertical field is nearly parallel at the outer region of the plasma, it will begin to curve in the wrong direction if one tries to increase e and S further. Therefore, using the criterion $n > 0$, the values $e = 2$ and $S = 1.6$ are the upper limits we can use for the UWMAK-III case. Another interesting point to note from this study is that a plasma like UWMAK-III with two stagnations points will have the unique advantage of providing both a stable elongated plasma and a divertor. It is therefore a good theoretical model for further study of the MHD stability of tokamaks.

The stability of the plasma against radial displacements and flipping is insured by the fact that $q(\Psi)$ is greater than q_h and q_f. To test for stability to vertical displacements, we consider a flux surface in the neighborhood of the magnetic axis for which $e = 1.4$ and $\beta_\theta = 1.2$. The corresponding value of e_{cr} is approximately 1.5 using the results in Ref. 14. Therefore $e < e_{cr}$ and

the plasma is stable with respect to vertical displacements.

The stability criteria D_I and D_R are given by the solid curve and dashed curve, respectively, in Fig. 6. The values of D_I and D_R are negative implying that localized modes are stable. Negative values of D_R provide strong stabilization for the tearing mode.

The critical β value estimated from Ref. 19 is 0.047 for an aspect ratio of 3, an elongation factor, e, of 2, and $\overline{\beta_\theta} = 1$. If we take $q = 3.5$ at the flux surface closest to the separatrix, we find

$$\beta = \left(\frac{S}{Aq}\right)^2 \overline{\beta_\theta} \simeq 0.032$$

for UWMAK-III and this is less than the critical β.[19]

The toroidal field in the vacuum and in the plasma are shown by dashed and solid curves in the upper part of Fig. 4. The diamagnetic effect is small, about 7%. The value of B_ϕ at the magnetic axis is reduced by 0.25 T. This means higher powers are needed when R. F. heating is used.[22] As useful information for R. F. heating studies, we present in Fig. 7 the resonance surfaces (i.e. the contours of constant $|B|$) as solid curves and the flux surfaces as dashed curves.

B. Analysis of a TCT-Tokamak Engineering Test Reactor

A preliminary study has been made on a smaller device, a reactor of special interest for use as a Tokamak Engineering Test Reactor (TETR)[4] based on the two energy component approach.[3] The major parameters of this conceptual device are listed in Table III[4] and a flux plot is shown in Fig.8. The values of D_I, D_R and q are shown in Fig. 9 while the vacuum field is given by Fig. 10. The profile of P and j_ϕ are shown in Fig. 11 while Fig. 12

shows the coil arrangement. The plasma parameters are I_p = 2.4 MA, R_o=3.05m, a=0.5m, B_o=4.0T and $\overline{\beta_\theta}$=3.5. The pressure profile is nearly parabolic and the current profile is almost linear. The plasma height to width ratio is 2.5 and the shape factor, S, is 1.8. From Fig. 7 one can see that $q(\Psi)>1$ and that D_R and D_I are negative. Thus, the plasma should be stable against localized modes. On the other hand, the vacuum field has the wrong curvature and the decay index is negative. This means that the plasma would have to be stabilized against rigid vertical displacements by a feedback system.

One difficulty in the design of such a small reactor is that the external coils are placed outside the blanket region far from the plasma. They are therefore not highly effective in controlling the plasma shape. Further investigations are required to study the equilibrium and stability of such a plasma using other pressure and current profiles. It is also necessary to examine the stability of this smaller plasma to modes other than localized ones.

IV. Scaling and Engineering Problems

The possibility of scaling the specific designs developed in section III has been studied. It appears indeed possible with slight modification to find plasmas of similar cross section for larger size tokamaks. An example is one with R_o=9.2m, I_p=16.6MA, a=2.8m, b=5.6m, B_o=4.0T and $\overline{\beta_\theta}$=2.2. It is also possible, though more difficult, to scale to smaller devices such as the TETR discussed in the previous section.

The findings presented in the last section clearly indicate that the ultimate plasma shape is strongly influenced by actual reactor engineering constraints such as the blanket and shield thickness. These constraints have been carefully included in the UWMAK-III study and Fig. 1 shows the vertical field coil arrangement, the blanket region, and the toroidal field coil. Another well known constraint is that the maximum toroidal field, B_{max}, at the inner magnet

surface is limited when the coil is supperconducting. In the UWMAK-III design, B_{max} is limited to 8.75 T at R_{in} = 3.75m. The space left for the blanket and shield between R_m and R_1 is about the minimum possible, 1.3m.

Acknowledgement

We are indebted to R. C. Grimm of the Princeton Plasma Physics Laboratory for making the MHD code available. The code was initially converted for use on the UNIVAC-1110 computer at Wisconsin by Sam Dahled. We also acknowledge stimulating discussions with J. L. Johnson, R. C. Grimm and K. Weimer. This research was partially supported by the Electric Power Research Institute.

References

1. T. Ohkawa, T. H. Jensen, Plasma Physics 12, 789(1971).

2. J. File, R. G. Mills, J. Sheffield, IEEE Transaction on Nuclear Science NS-18, 277 (1971).

3. J. M. Dawson, H. P. Furth, F. H. Tenney, Phys. Rev. Letts. 26,1156(1971).

4. R. W. Conn, D. L. Jassby, "A Tokamak Engineering Test Reactor" Princeton Plasma Physics Laboratory Report, MATT-1155 (Aug., 1975). To be published in Proc. International Conf. on Radiation Test Facilities for the CTR Surface and Materials Program (ERDA,1975).

5. University of Wisconsin Fusion Feasibility Study Group, R. W. Conn, et al. "The UWMAK-III Tokamak Reactor Design," Univ. of Wisconsin Report FDM-150 To be published.

6. Y. Suzuki, A. Kameayi, H. Ninomiya, M. Masuzaki, and H. Toyama, Proc. 5th IAEA Conf. on Plasma Phys. and Cont. Nucl. Fus. Research, 1974, (IAEA, Vienna, 1975) Vol. I, p. 411.

7. V. D. Shafranov, Review of Plasma Physics, (Consultants Bureau, New York) (1966), Vol. 2, p. 103.

8. John M. Greene, John L. Johnson, and Katherine Weimer, Phys. Fluids, Vol. 14, 671 671 (1971).

9. V. S. Mukhovatov, V. D. Shafranov, Nuclear Fusion 11, 605 (1971).

10. S. Yoshikawa, Phys. Fluids 7, 278 (1964).

11. M. S. Chance, R. L. Dewar, A. H. Glasser, J. M. Greene, R. C. Grimm, S. C. Jardin, J. L. Johnson, B. Rosen, G. W. Sheffield, and K. E. Weimer, Proc. 5th IAEA Conf. on Plasma Phys. and Cont. Nucl. Fus. Research, 1974, (IAEA, Vienna, 1975) Vol. I, p. 463.

13. L. E. Zakharov and V. D. Shafranov, Sov. Phys. Tech. Phys 18, 151 (1973).

14. E. Rebhan, Nuclear Fusion 15, 277 (1975).

15. M. D. Kruskal, J. L. Johnson, M. B. Gottlieb, and L. M. Goldman, Phys. Fluids, 1, 421 (1958).

16 V.D. Shafranov, Plasma Physics and the Problem of Controlled Thermonuclear Reactors (Pergamon, Oxford, 1969), Vol. 2, p. 197.

17. J. L. Johnson, J. M. Grene, Plasma Physics 9, 611 (1967).

18. A. H. Glasser, J. M. Greene, J. L. Johnson, submitted to Physics of Fluids.

19. J. P. Freidberg, W. Grossmann, Los Alamos Scientific Laboratory Report, LA-UR-75-416 (1973).

20. R. C. Grimm, J. M. Greene, and J. L. Johnson, to be published in Computational Physics, Vol. 16.

21. K. E. Weimer, E. A. Frieman, and J. L. Johnson, Plasma Phys. Vol. 17, 645 (1975).

22. J. E. Scharer, University of Wisconsin, private communication.

Table I

Plasma Parameters of UWMAK-III (5)

R_o = 8.1 m	I_p = 15.8 MA
B_o = 4.05 T	$\overline{\beta_\theta}$ = 2.2
R_{in} = 3.75 m	$q_* \cong$ 3.5
B_{max} = 8.75 T	$q_o \cong$ 1.0
R_m = 9.0 m	a = 2.7 m
R_j = 10.0 m	b $\cong$ 5.4 m
Δ_m = 0.8 m	S $\cong$ 1.6
Δ_j = 1.2 m	b/a = 2.0

Table II

External Coil Parameters of UWMAK-III

	Z(m)	R(m)	I(MA)
D_o	9.0	6.8	15.50
D_1	0.0	3.9	.40
D_2	1.0	3.9	.40
D_3	4.5	4.0	2.00
D_4	5.5	4.6	-0.60
D_5	9.0	3.9	-1.2
D_6	9.5	5.9	+2.2
D_7	10.0	8.8	-1.53
D_8	9.3	8.8	-1.65
D_9	9.9	8.8	-1.10
D_{10}	7.7	8.9	-1.60
D_{11}	7.5	9.3	-1.62
D_{12}	7.3	10.8	-1.55
D_{13}	6.8	11.8	-1.60
D_{14}	5.3	12.8	-1.65
D_{15}	4.3	13.0	-1.65
D_{16}	2.3	13.5	-1.52
D_{17}	0.0	13.5	-1.52

Table III

Plasma Parameters of a Tokamak Engineering Test Reactor[4]

R_o	3.05 m
a	0.50 m
A	5.56
b	1.25 m
b/a	2.5
S	1.8
B_o	4.0 T
I_p	2.4 MA
$\overline{\beta_\theta}$	3.5
q	2.5

Table IV

External Coil Arrangement for TETR

Coil No.	R(m)	Z(m)	I(MA)
D_1	1.8	0.8	0.2
D_2	2.4	2.7	3.9
D_3	3.5	3.5	-1.3
D_4	3.0	4.0	-8.4
D_5	4.5	2.4	-1.3
D_6	5.0	1.7	1.9
D_7	5.5	1.5	-1.2
D_8	6.0	0.0	-4.1

Figure Captions

Fig. 1. Cross-sectional view of the conceptual Tokamak fusion reactor design, UWMAK-III.

Fig. 2. Plot of surfaces of constant Ψ for UWMAK-III.

Fig. 3. Vacuum vertical field for maintaining the equilibrium plasma column of UWMAK-III.

Fig. 4. Plot of constant current density j_ϕ contour. The magnetude of j_ϕ increases from the plasma surface and then peaked at $R_j \cong 10$ meters.

Fig. 5. Plots of p (solid curve) and j_ϕ (dashed curve) in the lower part of the graph. Plot of toroidal field B_ϕ in the vacuum and in the plasma in the upper part of the graph respectively.

Fig. 6. Plots of the stability criteria D_I, D_R and safety factor q as functions of Ψ for the equilibrium configuration of Fig. 1.

Fig. 7. Plots of constant $|B|$ contours and some constant Ψ surfaces for the equilibrium plasma of Fig. 1. The values of $|B|$ vary in units of 0.2T from the left-most contour, where the value is 6.0T. The last contour on the right has $|B|$ equals to 3.3T.

Fig. 8. Plot of surfaces on constant Ψ for the Tokamak Engineering Test Reactor TETR.

Fig. 9. Vacuum vertical field for maintaining the equilibrium plasma column of TETR.

Fig. 10. The stability criteria D_I, D_R and safety factor q as function of Ψ for the equilibrium configuration of Fig. 1.

Fig. 11. Plots of pressure profile and current profile for TETR.

Fig. 12. External coil arrangement for the equilibrium configuration of Fig. 8.

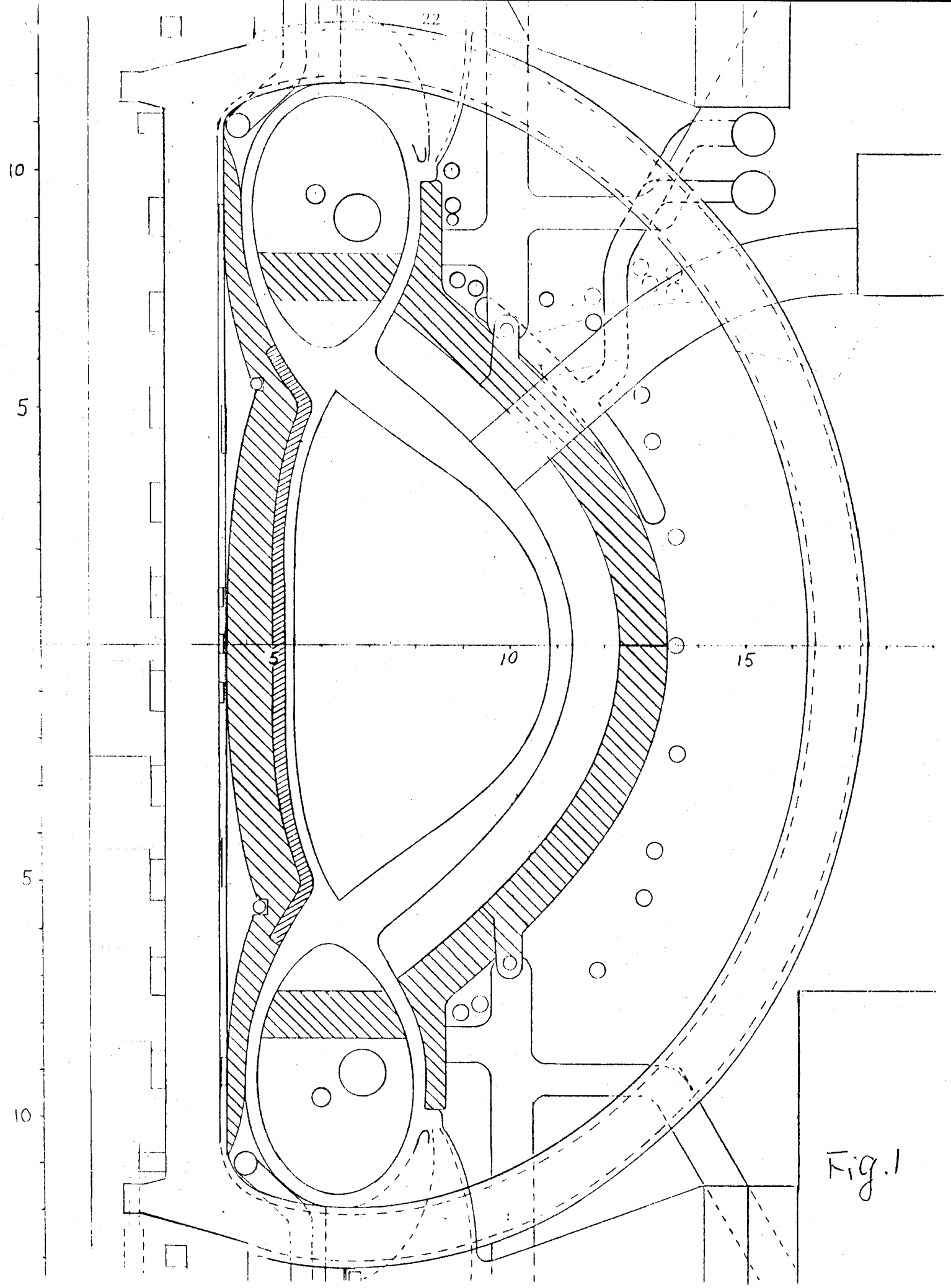

Fig. 1

Fig. 2

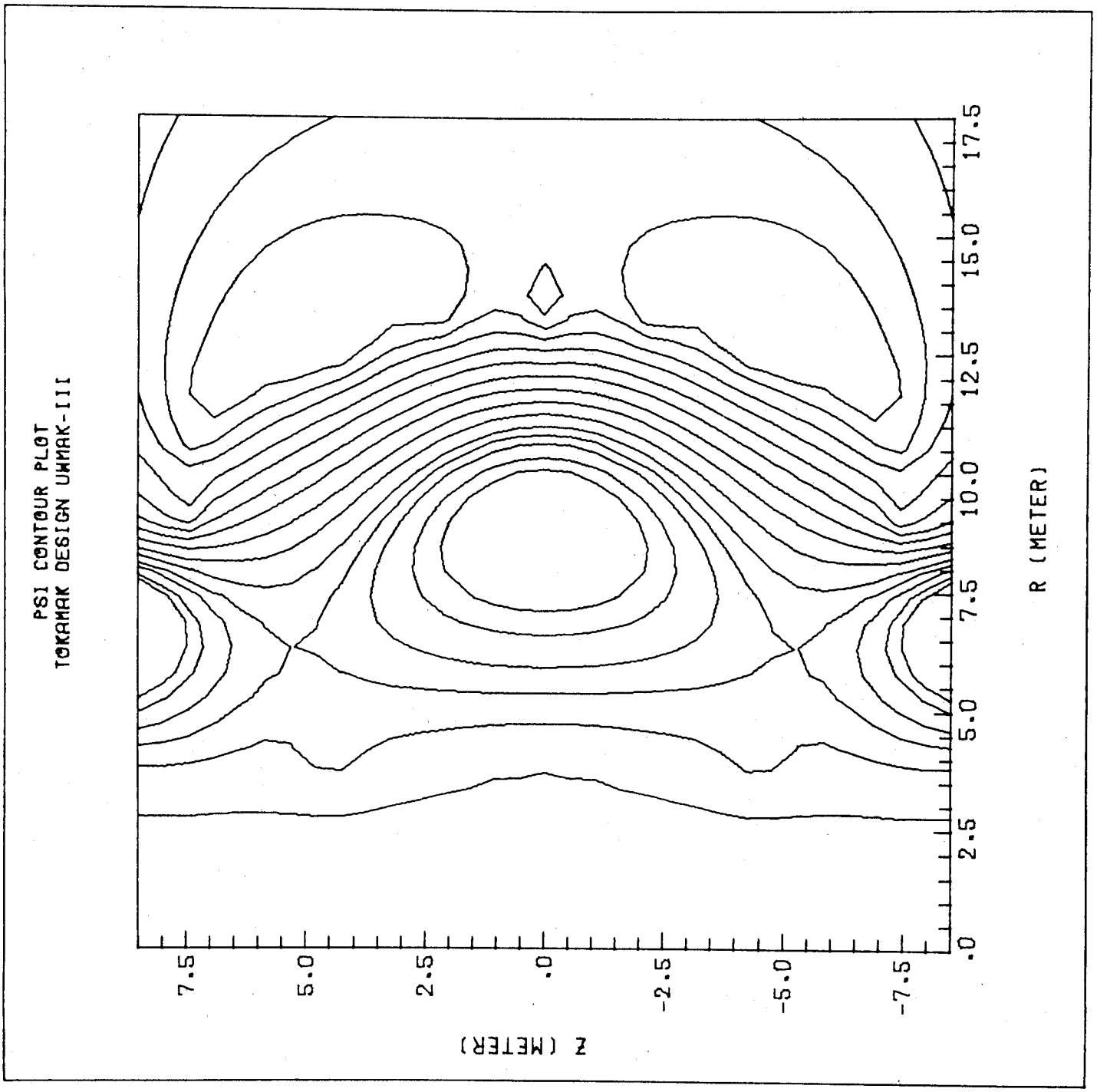
PSI CONTOUR PLOT
TOKAMAK DESIGN UWMAK-III
Z (METER)
7.5
5.0
2.5
.0
-2.5
-5.0
-7.5
R (METER)
.0
2.5
5.0
7.5
10.0
12.5
15.0
17.5

Fig. 3

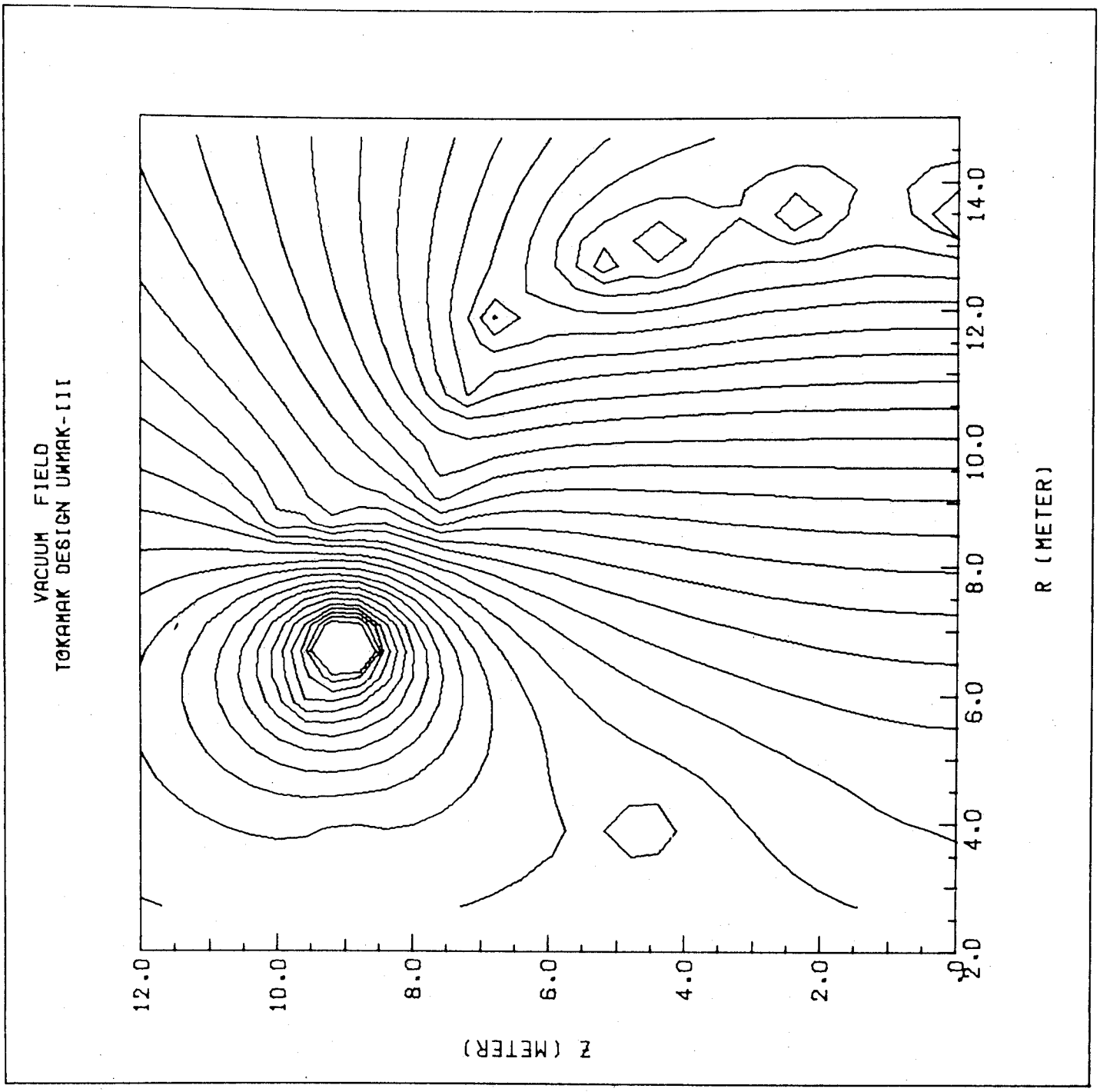
VACUUM FIELD
TOKAMAK DESIGN UWMAK-III
Z (METER)
12.0
10.0
8.0
6.0
4.0
2.0
0
2.0
4.0
6.0
8.0
10.0
12.0
14.0
R (METER)

Fig. 4

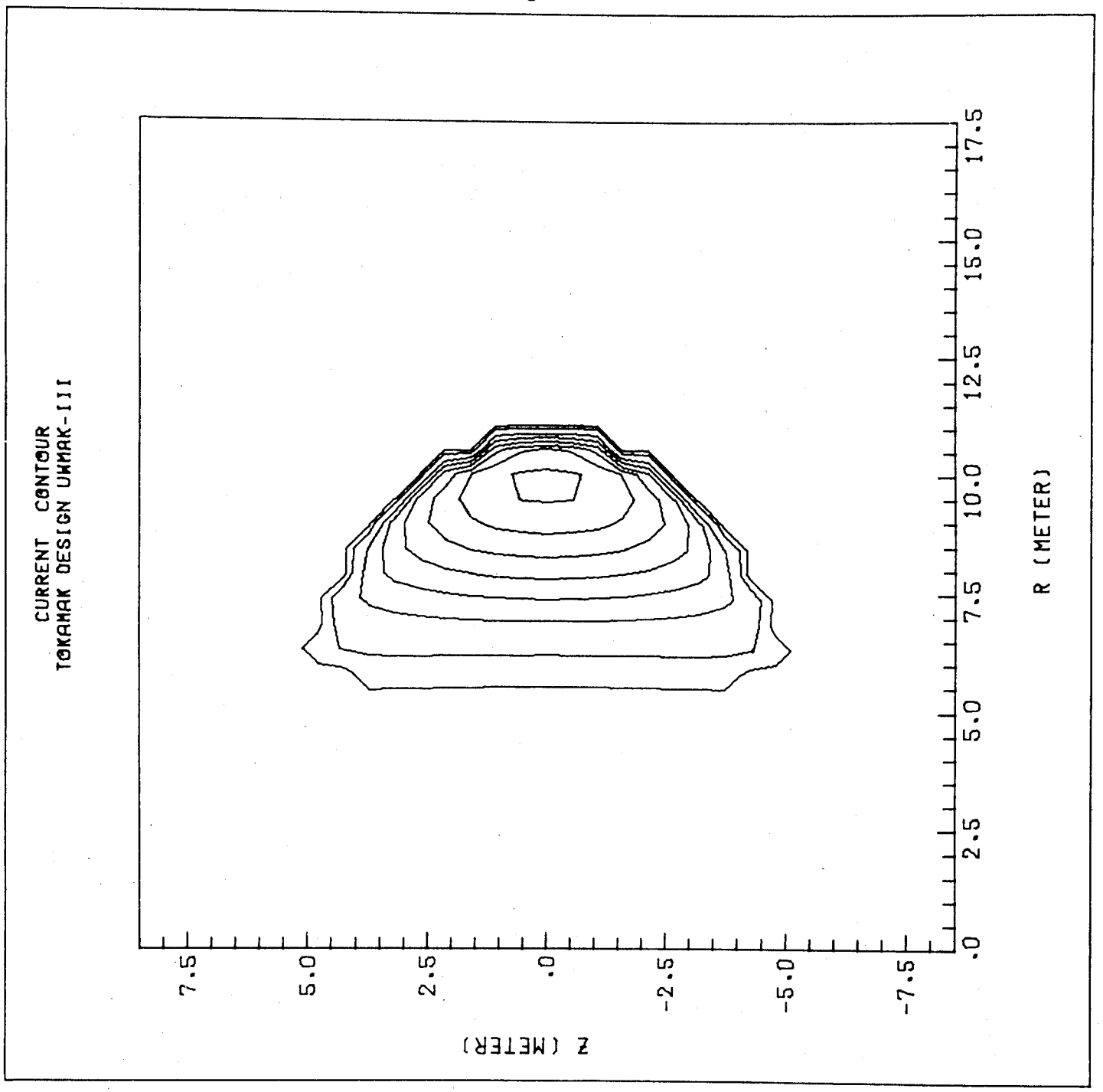
CURRENT CONTOUR
TOKAMAK DESIGN UWMAK-III
R (METER)
Z (METER)
17.5
15.0
12.5
10.0
7.5
5.0
2.5
.0
7.5
5.0
2.5
.0
-2.5
-5.0
-7.5

Fig. 5

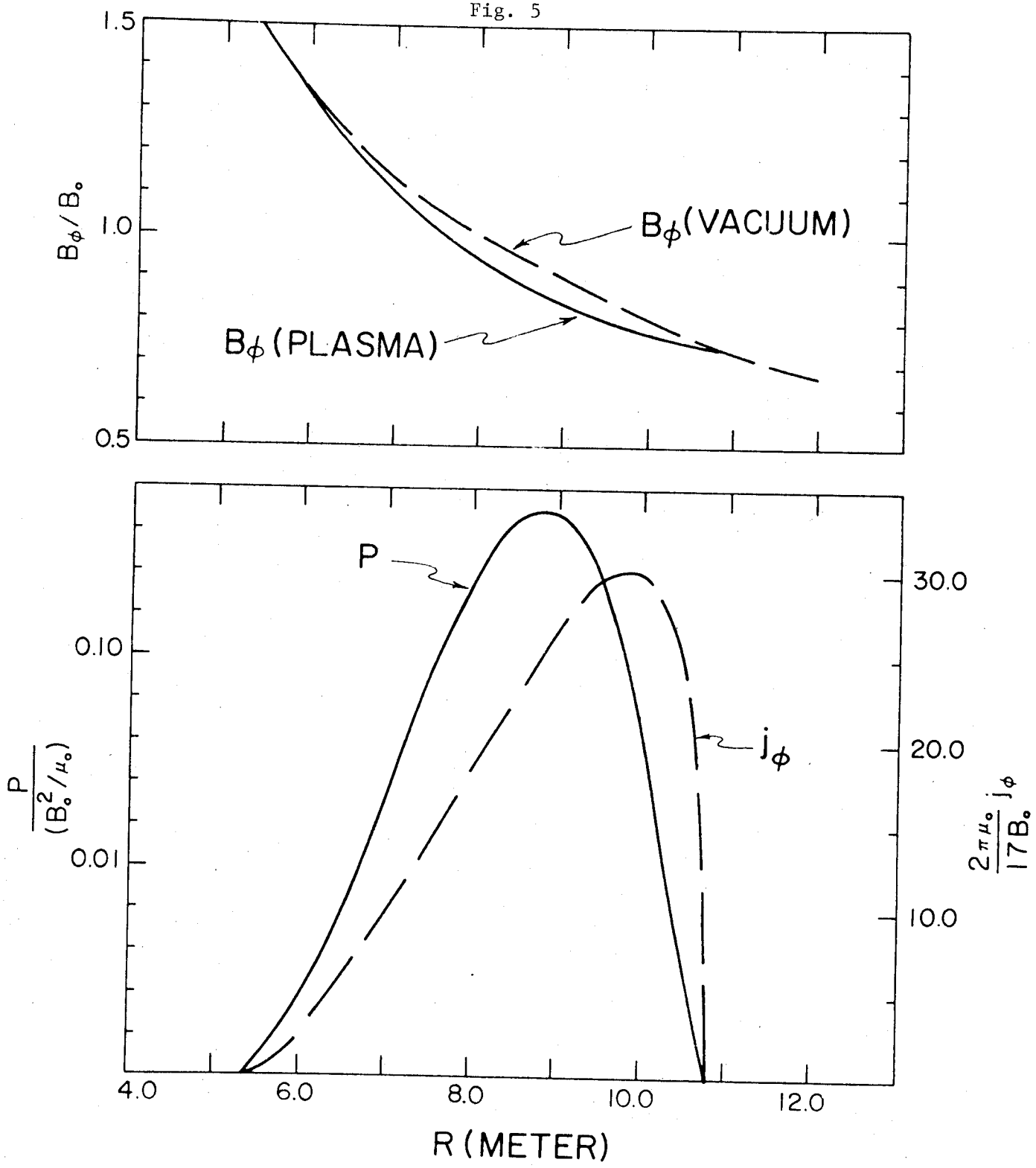
1.5
1.0
0.5
$B_\phi / B_\circ$
B_ϕ(VACUUM)
B_ϕ (PLASMA)
P
j_ϕ
0.10
0.01
$\frac{P}{(B_\circ^2/\mu_\circ)}$
30.0
20.0
10.0
$\frac{2\pi\mu_\circ}{17 B_\circ} j_\phi$
4.0
6.0
8.0
10.0
12.0
R (METER)

Fig. 6

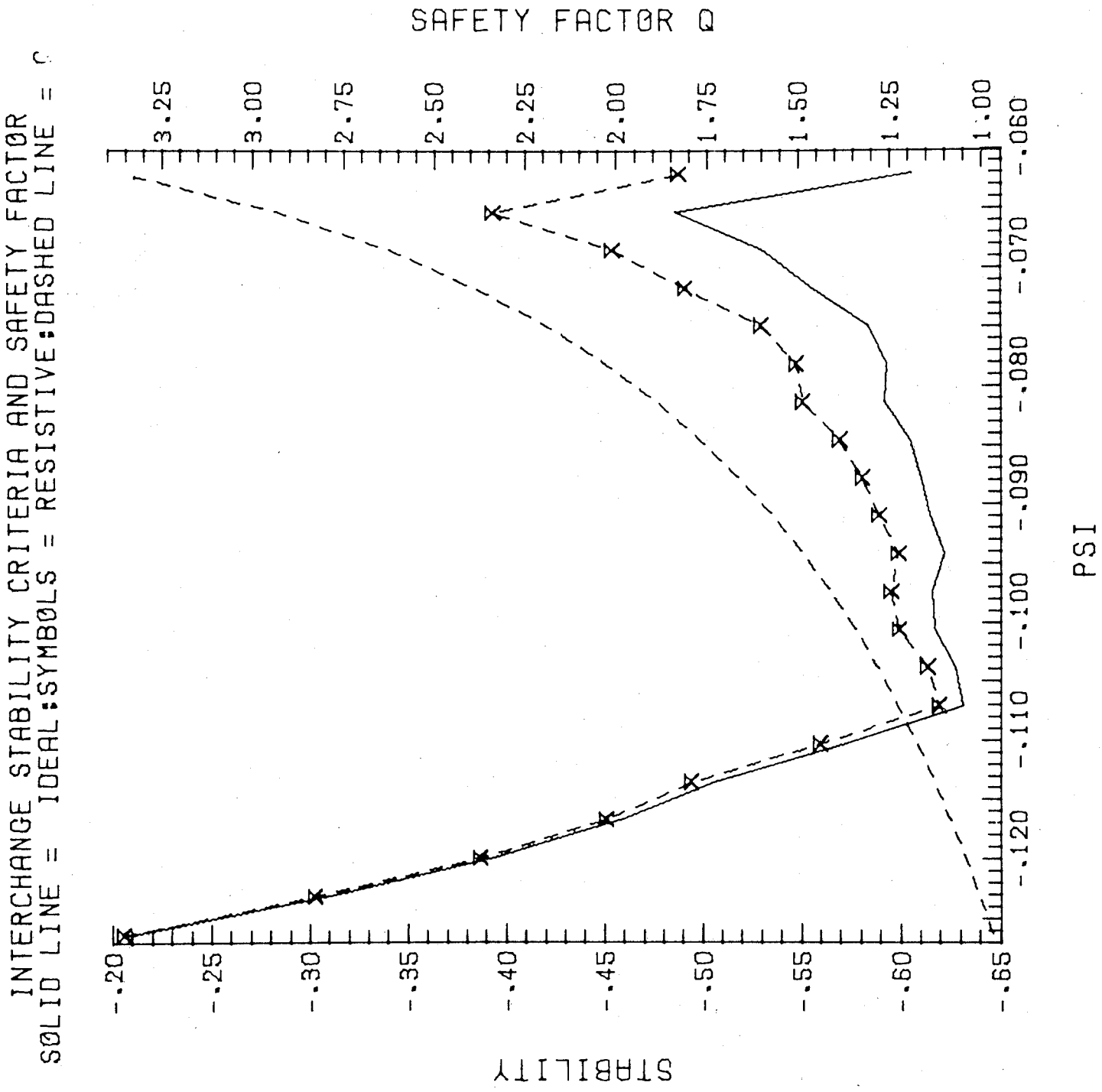
SAFETY FACTØR Q
INTERCHANGE STABILITY CRITERIA AND SAFETY FACTØR
SØLID LINE = IDEAL:SYMBØLS = RESISTIVE:DASHED LINE = C
3.25
3.00
2.75
2.50
2.25
2.00
1.75
1.50
1.25
1.00
-.060
-.070
-.080
-.090
-.100
-.110
-.120
-.20
-.25
-.30
-.35
-.40
-.45
-.50
-.55
-.60
-.65
STABILITY
PSI

Fig. 7

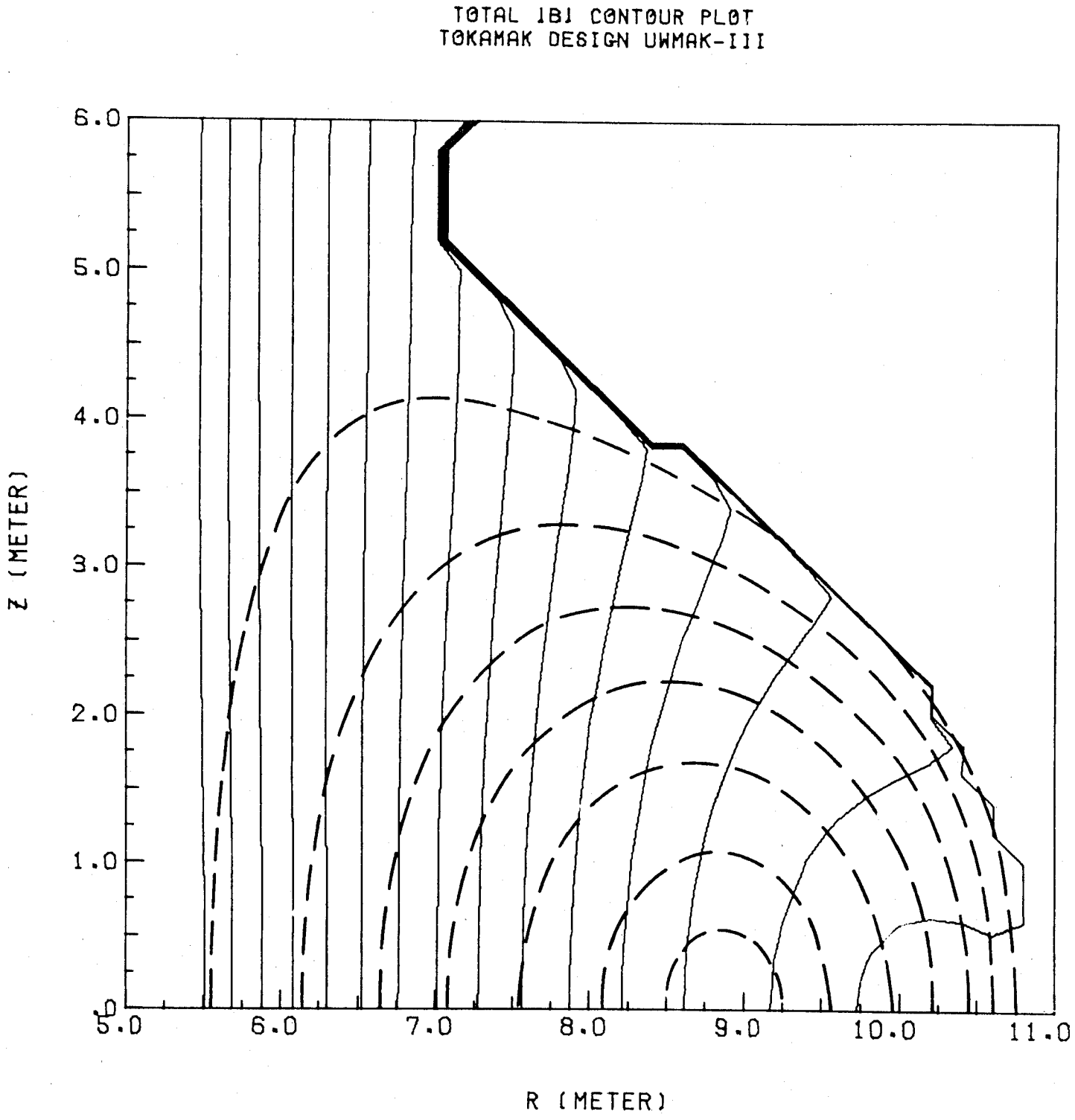
TOTAL |B| CONTOUR PLOT
TOKAMAK DESIGN UWMAK-III
6.0
5.0
4.0
3.0
2.0
1.0
0.0
Z (METER)
5.0
6.0
7.0
8.0
9.0
10.0
11.0
R (METER)

Fig. 8

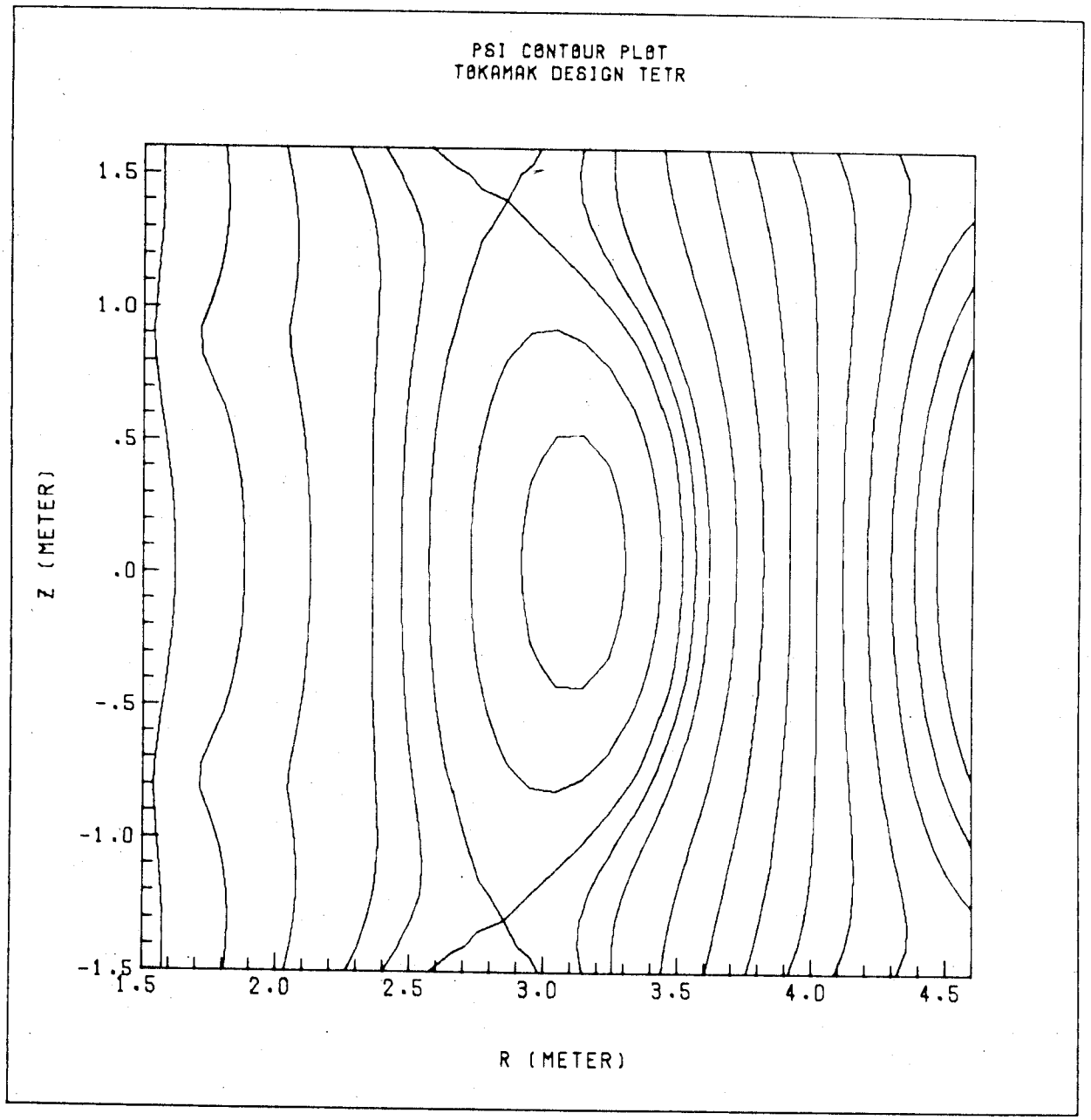
PSI CONTOUR PLOT
TOKAMAK DESIGN TETR
Z (METER)
1.5
1.0
.5
.0
-.5
-1.0
-1.5
1.5
2.0
2.5
3.0
3.5
4.0
4.5
R (METER)

Fig. 9

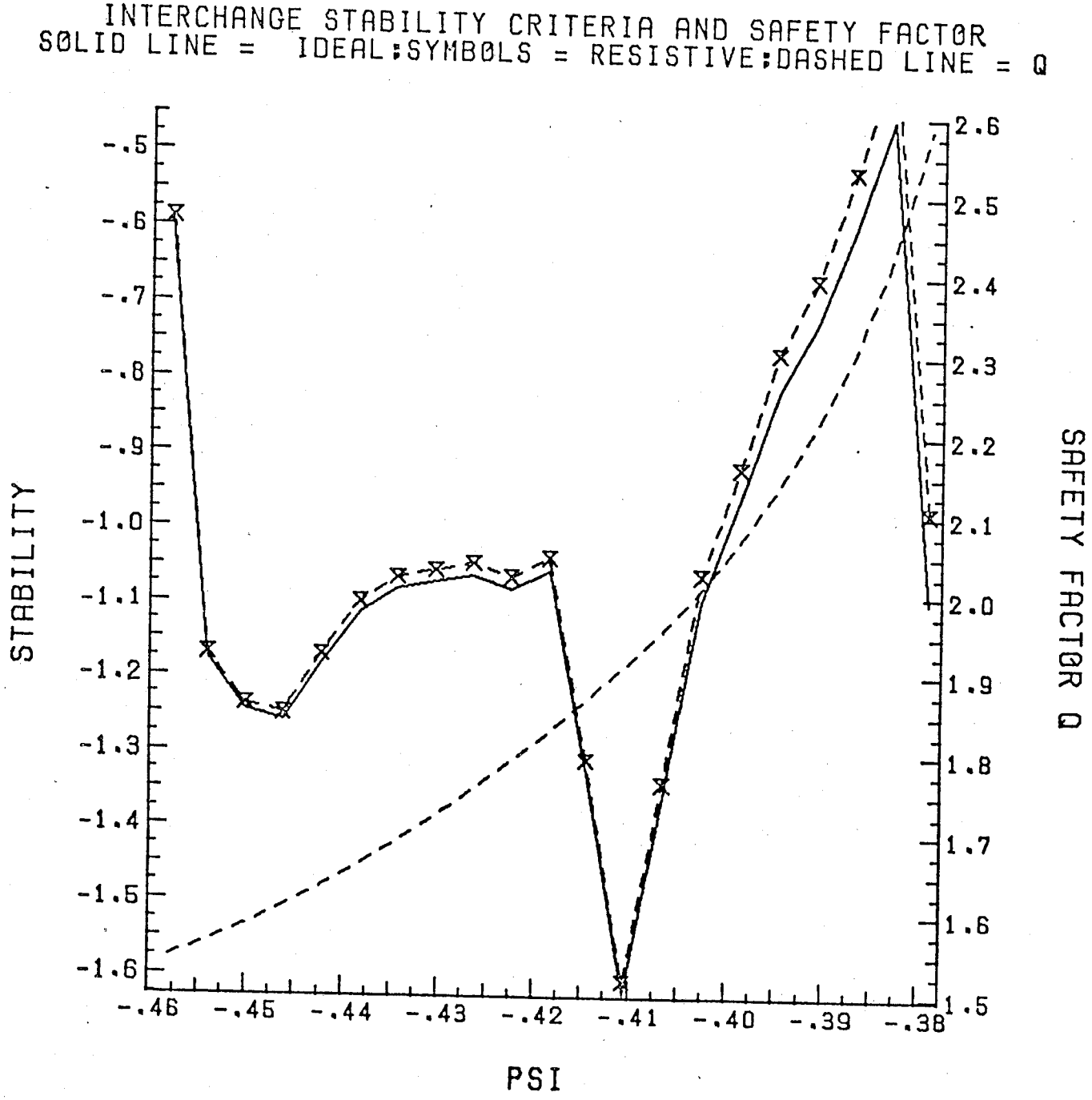
INTERCHANGE STABILITY CRITERIA AND SAFETY FACTOR
SOLID LINE = IDEAL;SYMBOLS = RESISTIVE;DASHED LINE = Q
STABILITY
SAFETY FACTOR Q
PSI
-.5
-.6
-.7
-.8
-.9
-1.0
-1.1
-1.2
-1.3
-1.4
-1.5
-1.6
2.6
2.5
2.4
2.3
2.2
2.1
2.0
1.9
1.8
1.7
1.6
1.5
-.46
-.45
-.44
-.43
-.42
-.41
-.40
-.39
-.38

Fig. 10

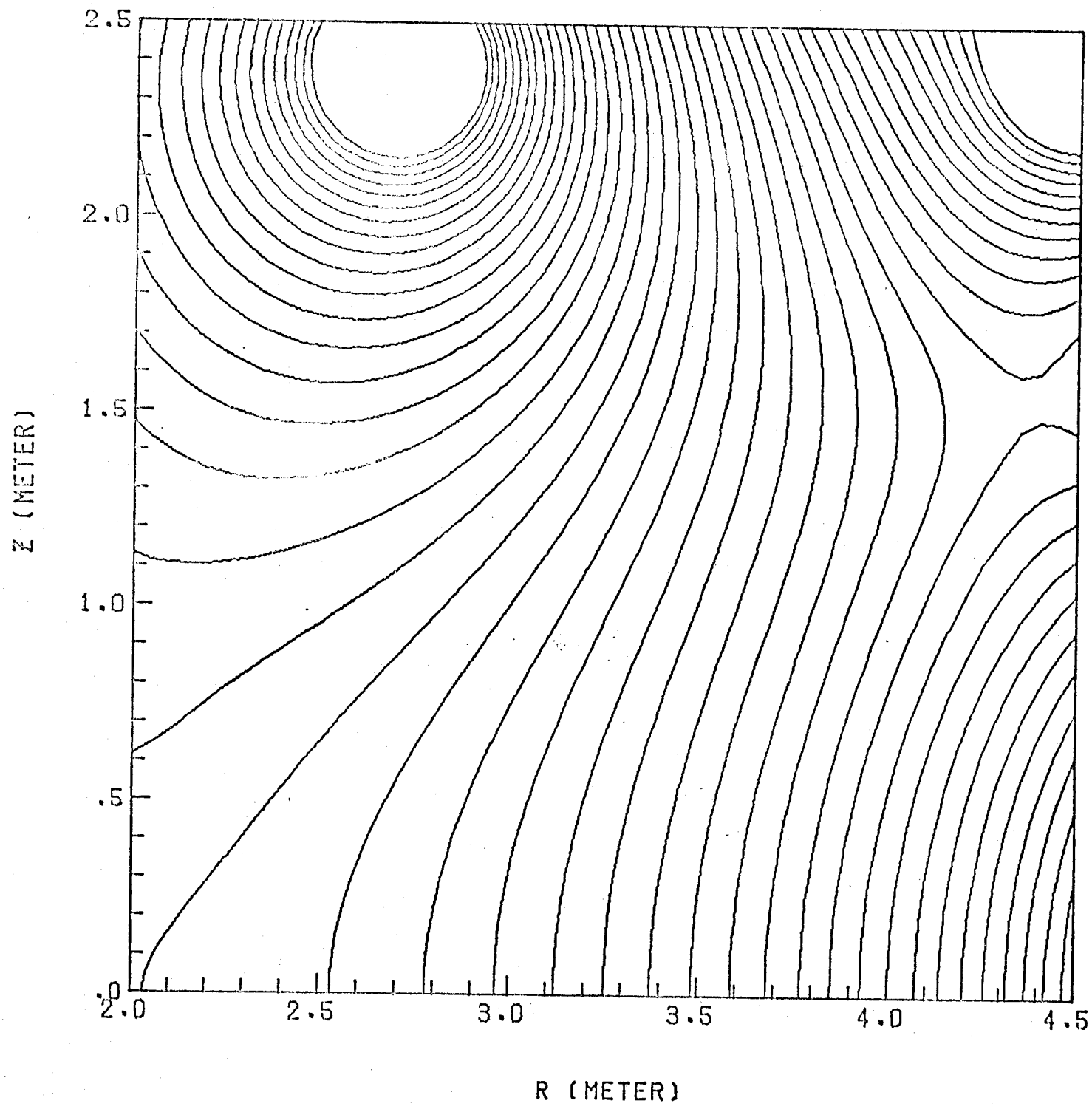

Fig. 11

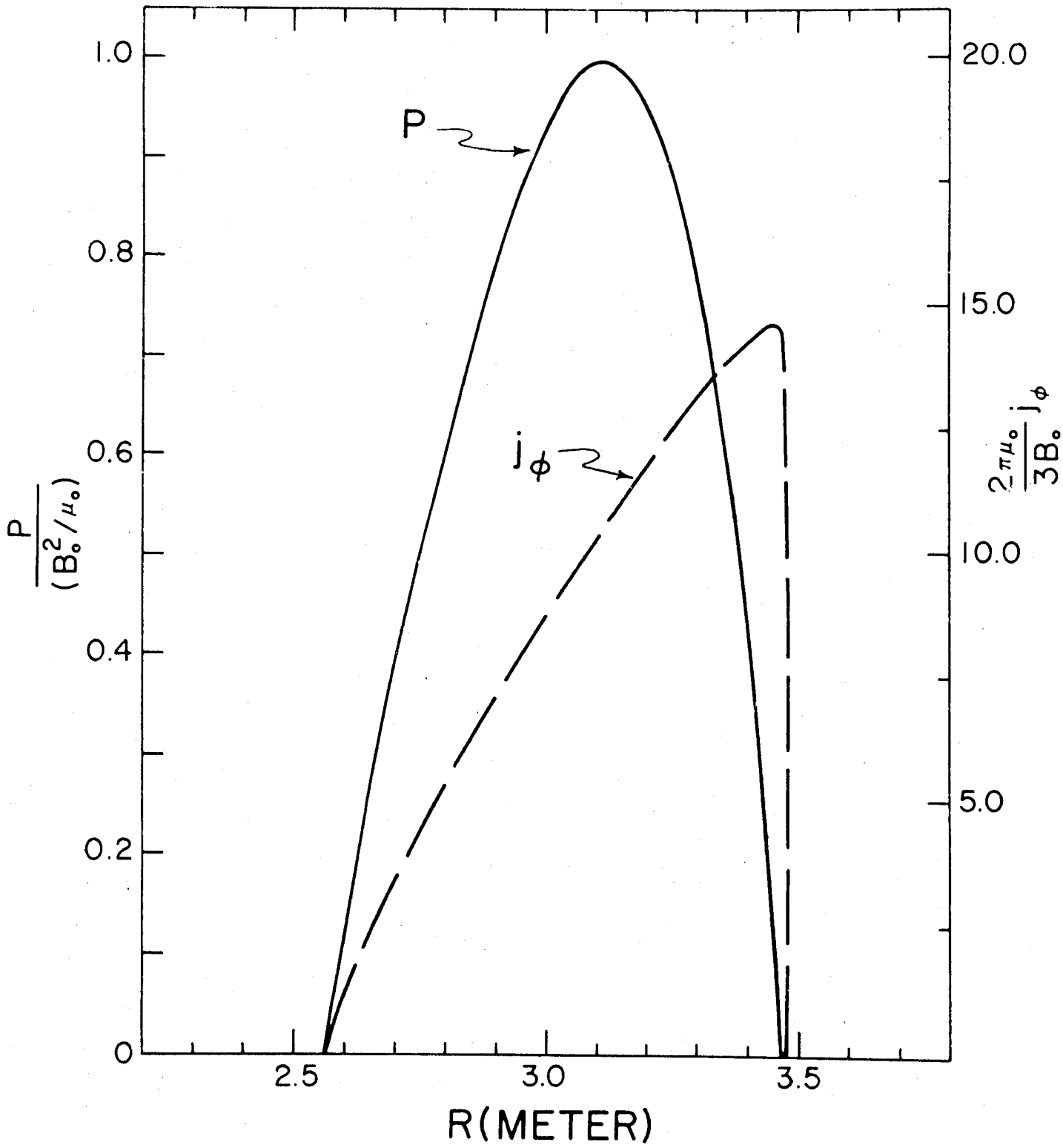
1.0
0.8
0.6
0.4
0.2
0
20.0
15.0
10.0
5.0
P
j_ϕ
$\frac{P}{(B_o^2/\mu_o)}$
$\frac{2\pi\mu_o}{3B_o} j_\phi$
2.5
3.0
3.5
R(METER)

Fig. 12

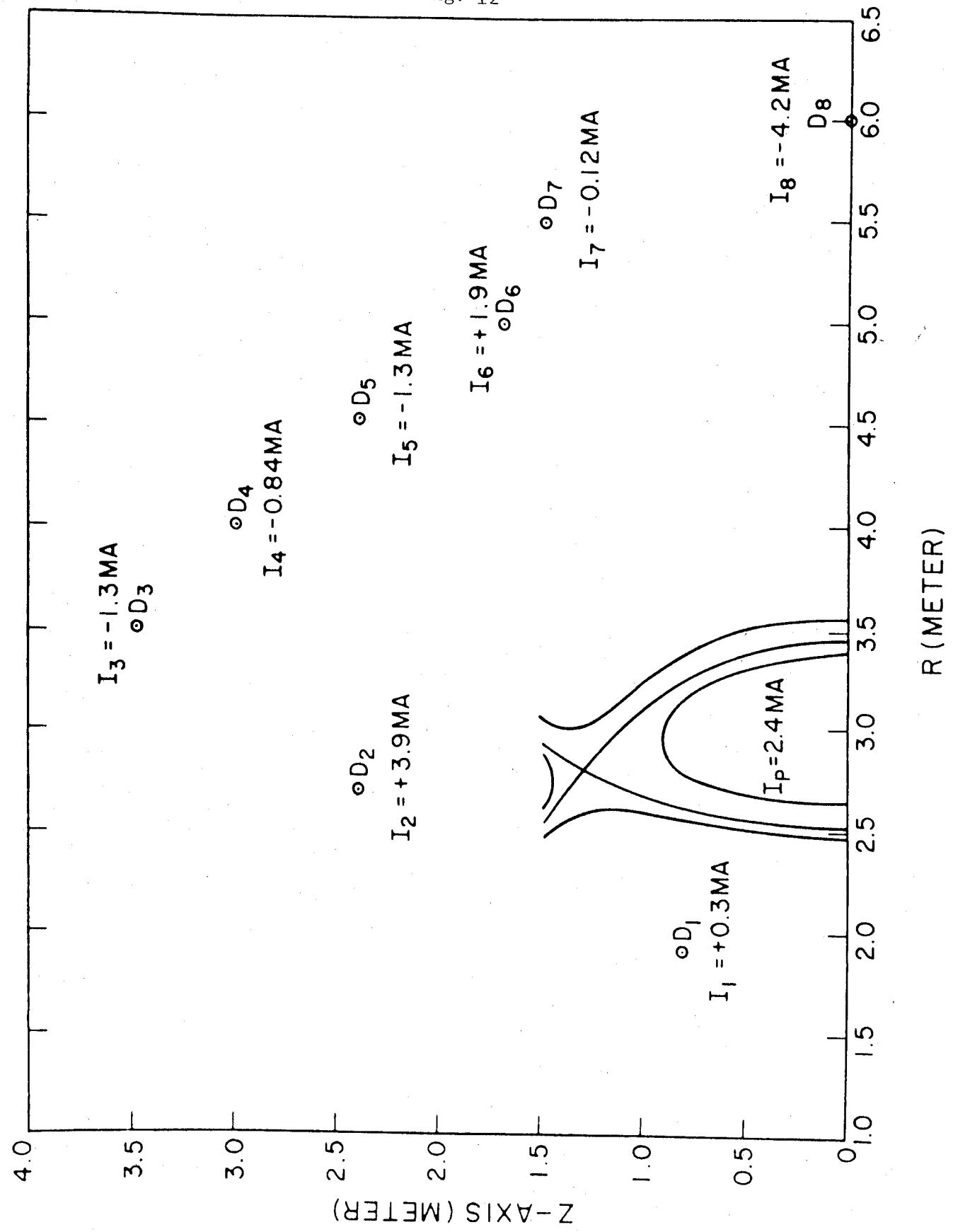
Z-AXIS (METER)
R (METER)
I_1 =+0.3MA
I_2 =+3.9MA
I_3 =-1.3MA
I_4 =-0.84MA
I_5 =-1.3MA
I_6 =+1.9MA
I_7 =-0.12MA
I_8 =-4.2MA
I_P=2.4MA
D_1
D_2
D_3
D_4
D_5
D_6
D_7
D_8